Extraordinary transmission from high-gain nanoaperture antennas

Edward C. Kinzel, Pornsak Srisungsitthisunti, Yan Li, Arvind Raman, and Xianfan Xu[a)]
School of Mechanical Engineering and Birck Nanotechnology Center, Purdue University, West Lafayette, Indiana 47907, USA

(Received 30 March 2010; accepted 4 May 2010; published online 26 May 2010)

This letter describes a bowtie nanoaperture antenna for coupling light to a subdiffraction limited near-field spot ($<\lambda/8$). The gain of the antenna is increased using a concentric grating structure to coherently diffract normally incident light toward the aperture. We experimentally demonstrate that the addition of the grating structure enhances the far-field transmission through the aperture by 6.9 times while the intensity at the near-field is increased more than 15 times. The nanoantenna is useful for applications including nanolithography and data storage. © *2010 American Institute of Physics*. [doi:10.1063/1.3436726]

Diffraction limits light from being focused to a spot smaller than $\lambda/2$ in far-field optics.[1] Transmission through a subwavelength hole of diameter d in a perfect electrically conducting (PEC) film scales with $(d/\lambda)^4$.[2] This is because no propagating mode exists for an aperture with a diameter less than 0.55 λ, the cutoff wavelength for a cylindrical waveguide.[3] Many applications require a bright near-field spot including nanolithography,[4] near-field imaging,[5] and heat-assisted magnetic recording.[6] Two approaches to improve the brightness of the subwavelength spot are to modify the shape of the aperture and to increase the amount of light refracted or scattered toward the aperture. Replacing the circular hole with a ridge aperture provides the same level of field confinement due to the much longer cutoff wavelengths.[3,7] Extraordinary transmission, where the total power diffracted exceeds the radiation incident on the open area of the aperture has been demonstrated with hole arrays[8] and by a hole surrounded with a concentric grating structure or "bull's eye."[9] This phenomenon has received significant research interest [e.g., Refs. 10 and 11], which results from a combination of diffractive, surface plasmon polariton (SPP), and scattering evanescent fields.[12]

This letter describes a bowtie aperture surrounded with concentric grating to form a high-gain nanoantenna. Previously, a single concentric ring was shown to enhance transmission of a "C" aperture by a factor of 2.45.[13] In our case, the grating structure functions similarly to a Fresnel zone plate with a zero working distance focusing light at its center. The focus of grating is diffraction limited but it couples to the aperture to confine the light to a $\lambda/8$ spot. Experimentally, we find that it transmits 15 times more than an isolated aperture without grating in the near-field, and 6.9 times more in the far-field. We discuss the fabrication procedure, experimental results, and the physical phenomena involved.

Figure 1 shows an scanning electron microscope (SEM) image and schematic of the antenna. It is formed by first depositing a 140-nm-thick indium tin oxide (ITO) film on top of a flat fused silica substrate using e-beam evaporation. The ITO serves as a transparent charge-dissipation layer for e-beam lithography (EBL). A 50-nm-thick hydrogen silsesquioxane (HSQ) is spun on top of the ITO. The HSQ acts as a negative tone resist and concentric rings are defined using EBL. A 100-nm-thick Al film is then deposited on top of the HSQ and ITO, also using e-beam evaporation. Finally, the bowtie aperture is formed using focused ion beam milling.

To investigate the performance of the antenna, we fabricated several similar structures with different grating periodicity. Prior to fabrication we used the frequency-domain finite-element method[14] to optimize the bowtie aperture dimensions along with the spacing and width of the rings of the grating. The antenna is illuminated with a normally incident plane wave. The width of the metal is taken as larger than the width of the slot in HSQ w_n, with $w_{n,e}=w_n+75$ nm, with the profile shown in Fig. 1. The electrical permittivity of SiO_2 and Al at $\lambda=632.8$ nm are taken to be $\varepsilon=2.12$ (Ref. 15) and $\varepsilon=-56.1+j20.9$,[16] respectively. The ITO film is modeled using $\varepsilon=3.76+j0.04$ [17]. We choose $r_0=387.5$ nm and $w_n=200$ nm except for the center post which is fixed at $w_0=100$ nm [see Fig. 1(c)]. The outline dimension of the bowtie aperture is kept constant at $a=b=350$. The spot size is determined by the gap in the ridge aperture, g. Due to the current profile of the ion beam, there is a taper to the aperture gap which measures ~80–90 nm at

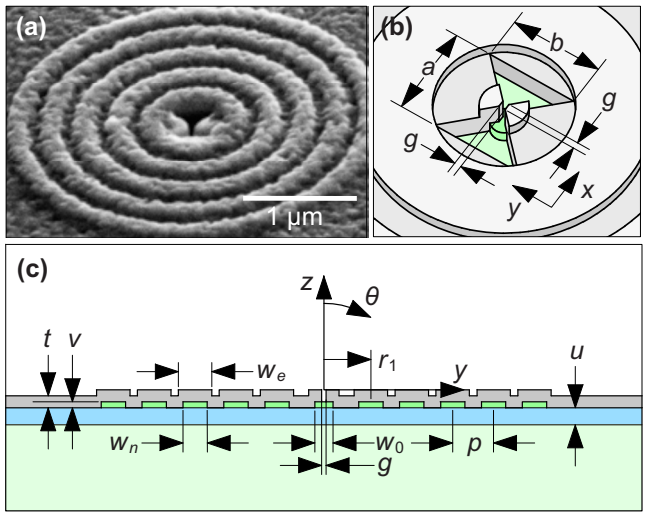

FIG. 1. (Color online) Structure geometry. (a) SEM image showing aluminum surface and bowtie aperture and [(b) and (c)] schematic of aperture and grating geometry.

[a)]Electronic mail: xxu@ecn.purdue.edu. Tel.: 1-765-494-5639. FAX: 1-765-494-0539.

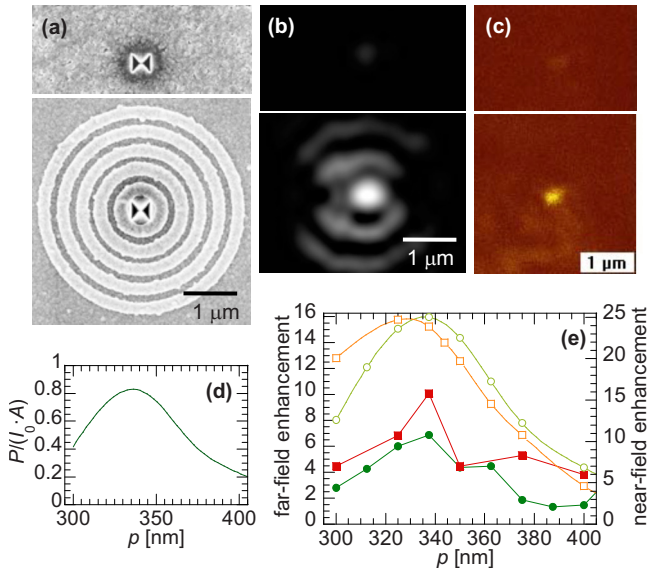

FIG. 2. (Color online) (a) SEM images of single bowtie and bowtie with grating, (b) far-field images of single bowtie without grating (top) and without grating (bottom), (c) NSOM images of single bowtie without grating (top) and bowtie with grating (bottom), (d) calculated ratio between the output power from the antenna/grating structure and the power incident on the open area of the bowtie aperture, and (e) enhancement achieved by adding the grating to the aperture, where the symbols □, ○, ■, and ● correspond to the enhancement simulated in the near-field, simulated in the far-field, measured in the near-field, and measured in the far-field, respectively.

its exit. Images of the fabricated bowtie apertures with and without grating are shown in Fig. 2(a).

Figures 2(b) and 2(c) show the near-field and far-field images of transmitted light from the bowtie aperture with and without grating. The far-field transmission is measured by placing the structure in a HeNe laser beam ($\lambda = 632.8$ nm, linearly polarized in the *y*-direction) and directly imaging the exit side of the film onto a charge coupled device camera as described in Ref. 18. The laser is linearly polarized across the gap of the bowtie [the *y*-direction in Fig. 1(b)]. The beam is not focused and its diameter is much greater than the size of the structures so that it can be treated as a uniform plane wave. Each data point is averaged over five antennas. Circular apertures with diameters of 100 and 200 nm are also fabricated. The transmission through the 100 nm hole is too small to measure. The maximum transmission through the antenna is obtained for the grating with pitch $p = 337.5$ nm, which is ~240× greater than that through a 200 nm hole even though the spot size from the antenna is smaller. The near field image is obtained using an aperture-based near-field scanning optical microscopy (NSOM).[5] We use a probe with an aperture of about 100 nm in diameter which limits our resolution since the NSOM signal represents a convolution between the probe resolution and the near field light intensity distribution. Using the Richardson–Lucy deconvolution method,[19] the near-field spot size is found to be less than 80 nm or less than $\lambda/8$.

The performance of the bowtie aperture with grating is first shown in Fig. 2(d) as the ratio of the total power transmitted from the antenna to the power of light incident on the open area of the bowtie antenna, P/I_oA. Note that this ratio is a measure of averaged intensity after the bowtie. There is strong spatial variation in the intensity after the bowtie as shown in previous studies of bowtie apertures (e.g., Ref. 4).

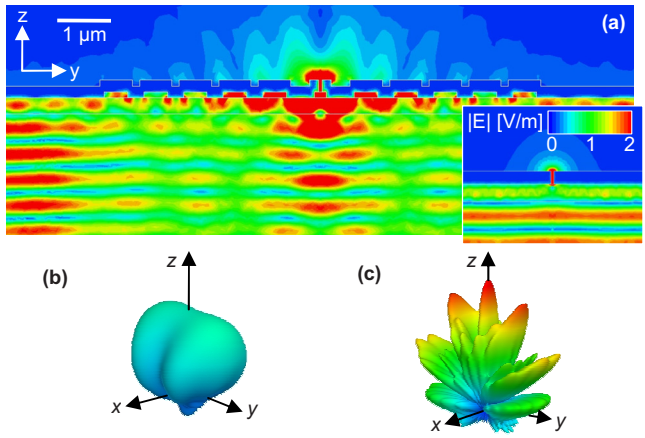

FIG. 3. (Color online) Numerical simulations. (a) Electric field on *yz* plane for bowtie antenna/grating structure—the inset shows the electric field for a bowtie without grating. Both images are saturated at 2 V/m. (b) and (c) Polar plots of the far-field angular distributions for bowtie aperture without the grating and bowtie antenna/grating antenna, respectively.

The peak intensity from the bowtie is located near the gap of the bowtie, which is much higher than the intensity averaged over the open area of the aperture.

Our main interest is to see how adding the grating structure can boost the transmission from the bowtie. Figure 2(e) shows the calculated and measured far- and near-field transmission with grating compared with bowtie apertures without grating. From the measurements, the addition of the grating enhances the far-field transmission by a factor of 6.9, and the measured near-field enhancement is about 15 times compared to the bowtie apertures without the grating. The reason that the near-field has a higher transmission is that energy can be stored in the near-field which does not radiate, which is also shown from the calculations in Fig. 2(e). Figure 2(e) also shows that the there is a about a factor of two discrepancy between the simulations and experimental results, which can come from imperfections in the fabricated structure.

Figure 3(a) shows the calculated electric field intensity on the antenna. The inset shows an identically sized aperture without the grating structure, where a standing wave is formed by the normal reflection from the Al film. The absence of the standing wave when there is a grating shows that the grating diffracts much of the light. Figure 3(c) shows a polar-plot of electric far-field for the bowtie antenna/grating structure. This calculated polar plot is consistent with what is observed in the far field as shown in Fig. 2(b). On the other hand, the bowtie antenna without grating structure produces a single spot in the far-field, which is seen in both measurement [Fig. 2(b)] and calculation [Fig. 3(b)].

Some physical insight can be gained from conventional optics. The scattered light can interfere to form diffraction orders according to the following:[1]

$$p(\sin\theta_m + \sin\theta_i) = m\lambda, \tag{1}$$

where p is the grating periodicity, m the diffraction order, and θ_m and θ_i the angles of incidence and diffracted light, respectively. For $\theta_i = 0°$, the first diffraction order lies along the surface, $\theta_m = 90°$ when the periodicity of the structure approaches the wavelength (the Rayleigh–Wood anomaly). From Eq. (1), the first order diffraction occurs at p ~325 nm for ITO which generally agrees with the full-

wave simulation results in Fig. 2(d). Therefore, the fundamental mechanism behind the enhancement from the periodic structure is a grating phenomenon, which occurs even when the film is modeled as PEC (Ref. 20) as opposed to being plasmonic.

In summary, we have demonstrated a bright near-field spot using a bowtie aperture with a concentric grating structure. The far-field transmission through the aperture is enhanced 6.9 times with the addition of the grating structure, while the near field transmission is enhanced by a factor of 15. In our structure, the dominant mechanism for the transmission enhancement comes from the grating diffraction, while the SPP effect plays a minor role.

Support for this work, provided by the National Science Foundation (Grant Nos. DMI-0707817 and DMI-0456809) and the Defense Advanced Research Project Agency (Grant No. N66001-08-1-2037, Program Manager Dr. Thomas Kenny) is gratefully acknowledged.

[1]M. Born and E. Wolf, *Principles of Optics*, 7th ed. (Cambridge University Press, Cambridge, 1999).
[2]H. A. Bethe, Phys. Rev. **66**, 163 (1944).
[3]D. M. Pozar, *Microwave Engineering* (Wiley, New York, 1998).
[4]L. Wang, S. M. Uppuluri, E. X. Jin, and X. Xu, Nano Lett. **6**, 361 (2006).
[5]E. X. Jin and X. Xu, J. Microsc. **229**, 503 (2008).
[6]K. Şendur, C. Peng, and W. Challener, Phys. Rev. Lett. **94**, 043901 (2005).
[7]X. Shi and L. Hesselink, Jpn. J. Appl. Phys., Part 1 **41**, 1632 (2002).
[8]C. Genet and T. W. Ebbesen, Nature (London) **445**, 39 (2007).
[9]H. J. Lezec, A. Degiron, E. Devaux, R. A. Linke, L. Martin-Moreno, F. J. Garcia-Vidal, and T. W. Ebbesen, Science **297**, 820 (2002).
[10]L. Martín-Moreno, F. J. García-Vidal, H. J. Lezec, A. Degiron, and T. W. Ebbesen, Phys. Rev. Lett. **90**, 167401 (2003).
[11]T. Ishi, J. Fujikata, K. Makita, T. Baba, and K. Ohashi, Jpn. J. Appl. Phys., Part 2 **44**, L364 (2005).
[12]H. J. Lezec and T. Thio, Opt. Express **12**, 3629 (2004).
[13]Y.-C. Chen, J.-Y. Fang, C.-H. Tien, and H.-P. D. Shieh, Opt. Lett. **31**, 655 (2006).
[14]HFSS 12.1, Ansoft Inc., 2010.
[15]I. J. Malitson, J. Opt. Soc. Am. **55**, 1205 (1965).
[16]E. D. Palik, *Handbook of Optical Constants of Solids* (Academic, San Diego, 1998).
[17]S. Laux, N. Kaiser, A. Zoller, R. Gotzelmann, H. Lauth, and H. Bernitzki, Thin Solid Films **335**, 1 (1998).
[18]P. Srisungsitthisunti, O. K. Ersoy, and X. Xu, Appl. Phys. Lett. **90**, 011104 (2007).
[19]W. H. Richardson, J. Opt. Soc. Am. **62**, 55 (1972).
[20]F. J. García-Vidal, H. J. Lezec, T. W. Ebbesen, and L. Martin-Moreno, Phys. Rev. Lett. **90**, 213901 (2003).